

Stability of angular extrapolation methods for determining the deuteron asymptotic D -state to S -state ratio

J. T. Londergan and C. E. Price

Department of Physics and Nuclear Theory Center, Indiana University, Bloomington, Indiana 47405

E. J. Stephenson

Indiana University Cyclotron Facility, Bloomington, Indiana 47405

(Received 6 November 1986)

We review the current status of the extraction of the deuteron D -state to S -state ratio, η , from measurements of the tensor polarized cross section, σT_{22} , in elastic $d+p$ scattering. We examine various extrapolation techniques for obtaining η and conclude in several independent ways that such techniques suffer from large truncation errors. First we show that different methods for determining η give rise to very different results. Second, we use a theoretical model which estimates η to demonstrate the magnitude of the truncation error. Third, high-precision analyzing power data also generate large changes when compared with the results from earlier, less precise measurements. The original estimates of η appeared to agree with theory; we show that such agreement was fortuitous, and was the result of the simultaneous neglect of large Coulomb penetrability corrections and large truncation errors. We conclude that the uncertainty in η is considerably larger than was suggested by the errors quoted in the literature.

I. INTRODUCTION

In recent years there has been considerable interest in a precise determination of the asymptotic D - to S -state ratio η for the deuteron, especially since the D -state probability is now regarded as a highly model-dependent quantity.¹ Two methods have now emerged which potentially can yield this sort of information. One, based on a distorted-wave Born approximation (DWBA) analysis of sub-Coulomb (d,p) reactions on heavy targets,² gives the closely related parameter D_2 (Ref. 3). Refinements were made, both experimentally⁴ and theoretically,⁵ providing an average value for the D - to S -state ratio of $\eta = 0.0271 \pm 0.0008$. Recent improvements⁶ in the measurement of tensor beam polarization have led to a new value of $\eta = 0.0256 \pm 0.0004$. However, there is concern⁷ that channel coupling between the elastic and transfer reaction channels of the type presented in Ref. 5 may alter some of the corrections and change the value deduced for η .

The second method, first proposed by Amado, Locher, and Simonius⁸ (and subsequently refined⁹), extracts the asymptotic D - to S -state ratio by the angular extrapolation of the tensor polarized cross section σT_{22} in $\bar{d} + p$ elastic scattering. In this method, the measurements are reproduced by a polynomial series expansion in $z = \cos\theta_{c.m.}$. Then the polynomial is evaluated at the location of the neutron exchange singularity in the unphysical region where $z < -1$. There it equals the pole residue, which is proportional in lowest order to the D -state coupling constant. Division by the S -state coupling constant yields the D - to S -state ratio η . Subsequent measurements^{10,11} gave values for η that appeared to be relatively

constant with deuteron bombarding energy from 5 to 45.3 MeV, in accordance with the expectation that the value of this residue depended only on the structure of the deuteron. An extrapolation has also been made of the tensor polarized cross sections from the low energy ${}^2\text{H}(d,p){}^3\text{H}$ reaction,¹² with similar results.

In addition to these "direct" measurements of the parameter η , there are "indirect" values which can be inferred from the close connection between η and other deuteron observables, particularly the deuteron quadrupole moment Q . The close relation between η and Q has long been known,¹³ and useful summaries of our present knowledge of these observables are given in Refs. 14–17. Although short-range effects give some uncertainty in the indirect determination of η , it would be virtually impossible for any changes to be greater than about 10%. Therefore, we can ask the following questions.

- (1) Does the "direct" determination of η agree with the "indirect" constraints on η due to its relation with Q ?
- (2) Can the "direct" determination of η yield a value which is more precise than the value inferred from our knowledge of Q ?

Here we are mainly interested in the angular extrapolation method, particularly since it has been advertised as a "model-independent" determination of η .

Reference 14 contains a useful summary of the values of $\langle n \rangle$ which can be extracted by various techniques. Of these values, one obtains $\eta = 0.0263$ from the Paris potential.¹⁸ Klarsfeld *et al.*^{16,17} obtain limits $0.0261 < \eta < 0.0275$ by considering potential interactions which reduce to one-pion exchange (OPE) outside some radius

and are constrained to reproduce Q and the deuteron rms radius. Ericson and Rosa-Clot¹⁴ contend that the universal relation between Q and η suggests the very strong indirect relation $\langle \eta \rangle = 0.0264 \pm 0.0003$. Experimental analysis of polarized deuteron reactions by extrapolation or the equivalent "method of asymptotical coefficients" (discussed in Appendix B) have led to claims that such methods give a precise determination of $\langle \eta \rangle$. For example, Ref. 14 quotes values $\langle \eta \rangle = 0.0263 \pm 0.0009$ from $\vec{d} + p$ elastic scattering and $\langle \eta \rangle = 0.0272 \pm 0.0004$ from the ${}^2\text{H}(d,p){}^3\text{H}$ reaction. If such claims are correct, then the resulting value for η deserves considerable study. First, the extrapolation method would definitely provide the most precise direct determination of η . Second, if the value of η can truly be extracted to this precision, then one should pay very close attention to corrections and refinements to these techniques, at the level of 1% or smaller.

In this paper we carefully analyze the details of the extrapolation procedure. We conclude that the errors in this process are considerably larger than have been claimed in the literature. The reason for this, as we will demonstrate, is that the extrapolation procedure excludes certain errors ("truncation errors") when the uncertainty in η is calculated. We will demonstrate in two ways that the truncation errors tend to be large relative to the quoted errors. First, we will use a theoretical model¹⁹ to estimate the truncation errors, and we will compare these errors to those quoted for η . Second, we will examine a recent high-precision measurement of $\vec{d} + p$ scattering.²⁰ This measurement allows us to make an experimental estimate of some of the truncation error corrections to the value of η determined from previous experiments. Both the model and the high-precision experiment demonstrate that the published errors from the extrapolation method significantly underestimate the true error in this procedure; furthermore, we shall show that estimates of the truncation error provided by the model and by the precision data agree, and are consistent with other independent estimates of the truncation errors.^{21,22}

Unfortunately, our conclusions are negative: We find that the extrapolation method has considerably larger errors than have been claimed. However, since such claims continue to be made in the literature,^{23,24} and since considerable theoretical effort has been expended on the assumption that the published values and errors for η are accurate, we believe that it is worth the effort to correct this impression. This will require a fair amount of review, and a rather detailed discussion of the errors in this procedure.

In Sec. II we review the standard angular extrapolation technique. We will pay special attention to the errors inherent in this process, particularly the truncation error. We also mention the difficulties posed by the Rutherford singularity at forward angles in the $\vec{d} + p$ scattering. In Sec. III we present a model for the scattering amplitude which we have used to study the convergence of the polynomial series for $d + p$ scattering. We expand the scattering amplitude in terms of the nearest singularities in the complex variable z ,²⁵ and sum up these amplitudes with adjustable coefficients to reproduce the measured polar-

ized cross section. Section III briefly describes the choice of singularities for the model, the fitting procedure, and our conclusions. A full description of the model is given in Appendix A.

In Sec. IV we discuss two methods for removing the Rutherford singularity at $z=1$: suppression of the singularity in the extrapolation function, and conformal mapping of the data prior to extrapolation. We discuss in detail the advantages and disadvantages of both methods. An overview of these results, when compared with model values, provides an insight into the size of the truncation error. In Sec. V we compare the high-precision data of Casavant *et al.*²⁰ with the earlier measurements of $\vec{d} + p$ scattering, and with our model. This comparison also reveals that the truncation errors are large relative to the errors quoted in the literature. Also, by comparing our model (adjusted using the older data) with the more precise data, we show that our model is capable of predicting the contribution from higher-order terms in the polynomial series. In Sec. VI we compare different experimental results with one another, and comment on the present state of the data for these extrapolation procedures.

In Sec. VII we summarize our results and present our conclusions. In Appendix B we review the "method of asymptotical coefficients." This method has been presented as an alternative to the angular extrapolation model.^{23,26} We discuss briefly any advantages which this method might have in determining η .

II. REVIEW OF THE STANDARD ANGULAR EXTRAPOLATION TECHNIQUE

The techniques of angular extrapolation have been reviewed by Locher and Mizutani.²⁷ We review here the application of these techniques to the extraction of η from $\vec{d} + p$ scattering measurements.

The scattering amplitude is assumed to be analytic in the variable $z = \cos\theta_{c.m.}$, and thus completely specified by the locations of its singularities (branch cuts) and their residues (spectral functions). The residue for neutron exchange between two protons depends solely on the deuteron dnp vertex function; its value at the exchange pole is related to the deuteron coupling constant, or the asymptotic normalization of the deuteron wave function.²⁷ In the usual extrapolation analysis, this pole lies at

$$z_p = -\frac{5}{4} - \frac{9B}{4E_d}, \quad (1)$$

where B is the deuteron binding energy and E_d is the deuteron laboratory bombarding energy. The extrapolation function is

$$F(z) = p^2 \sigma T_{22} \frac{(z - z_p)^2}{1 - z^2}. \quad (2)$$

The factor $(z - z_p)^2$ removes the divergence associated with the neutron exchange singularity, making $F(z_p)$ finite. The second rank character of the tensor analyzing power T_{22} requires that the leading term in the residue contains one D -state dnp vertex function. Thus, $F(z_p)$ is proportional to the dnp D -state coupling constant in first order. Kinematic zeros in σT_{22} at $\theta = 0^\circ$ and 180° are re-

moved by the $1 - z^2 = \sin^2(\theta)$ factor in the denominator. Lastly, the square of the center-of-mass momentum, p , ensures that $F(z)$ is dimensionless.

At each deuteron bombarding energy, measurements of the cross section and tensor analyzing power are used to generate experimental values of the extrapolation function, $F(z)$. These values are then reproduced by a polynomial series of finite order whose coefficients are chosen to minimize the value of chi square based on the difference between the measurements and the extrapolation polynomial. One can write the function $F(z)$ as a power series containing two parts:

$$F(z) = \sum_{l=0}^L a_l P_l(z) + \sum_{l=L+1}^{\infty} a_l P_l(z) \equiv \bar{F}(z, L) + F_{\text{tr}}. \quad (3)$$

The polynomials $P_l(z)$ are l th order polynomials in z . The most useful basis functions are polynomials orthonormalized on the data (as will be shown at the end of this section). The first contribution to $F(z)$, which we have called $\bar{F}(z, L)$, can be measured experimentally. For any set of data, L is the maximum order which can be determined from the data (i.e., the order at which chi square per degree of freedom equals 1; or, the point where the chi square stabilizes as a function of increasing L). The coefficients a_l and their errors δa_l can be determined from the data for $l \leq L$. Additional terms are statistically insignificant in the physical region, and have customarily been omitted from the extrapolation procedure. Thus, the "truncation error" F_{tr} in Eq. (3) is the (unmeasurable) remainder term.

In the physical region $|z| \leq 1$, the truncation error is small and oscillatory. However, to determine the quantity η by extrapolation, we must extrapolate F to the unphysical angle z_p , where $z_p < -1$. Since the polynomials grow as z^l , high-order terms which might be very small in the physical region can become quite large in the unphysical region.

If the deuteron S -state vertex constant is known, then the D - to S -state ratio η can be extracted from⁹

$$\eta = -\frac{1}{P} \left[\frac{3}{128} \right]^{1/2} (1 - R\kappa)^2 F(z_p) = -\frac{0.0541}{P} F(z_p). \quad (4)$$

In Eq. (4), R is the triplet effective range in $n + p$ scattering, κ is the deuteron internal wave number, and P is the Coulomb penetrability, as calculated by Santos and Colby.^{28,29} P is given by the expression

$$P = \frac{4\pi\eta_C}{e^{4\pi\eta_C} - 1} \exp \left[4\eta_C \tan^{-1} \left[\frac{2p}{\kappa} \right] \right], \quad (5)$$

where η_C is the usual Coulomb parameter.

Since we cannot calculate the truncation correction to the extrapolation function F , $\bar{F}(z_p, L)$ is substituted for $F(z_p)$ when η is calculated through Eq. (4). There are thus two types of error associated with this approximation. First, there are the experimental errors, the errors in $\bar{F}(z_p, L)$ which arise from the uncertainties in the coefficients a_l extracted from the data in the physical region. Second, there is the truncation error, the error caused by

neglecting F_{tr} . In the published papers which employ angle extrapolation, *the quoted error is the experimental error only*. Clearly, this procedure underestimates the "true" errors in extrapolation; in the remainder of this paper we will give several estimates of the truncation error, and we will conclude that the truncation error is generally large relative to the quoted experimental error.

Angular distribution measurements of σT_{22} in deuteron-proton elastic scattering have been made at deuteron incident energies between 5 and 56 MeV. The measurements at 5, 7, 10, 13, and 20 MeV from Zürich (Ref. 11, and shown in Ref. 31), at 35 and 45.3 MeV from Berkeley (Ref. 10), at 56 MeV from Osaka (Ref. 30), and at 10 MeV from Wisconsin (Ref. 20) are the only ones available in tabular form with errors. The cross sections to complement the T_{22} measurements of Refs. 20 and 31 at 5–20 MeV are taken from Kocher and Clegg.³² The values of $F(z)$ at each energy are shown in Fig. 1, where a logarithmic scale is used to clarify the quality of the polynomial fit at all values of z . Because of the large number of data points, we have used the measurements at 10 and 45.3 MeV for detailed studies.

For each data set we have repeated the extrapolation procedure outlined above. The polynomial coefficients a_l of Eq. (3) were determined using matrix inversion techniques.³³ For this first stage, we used Legendre polynomials for expanding the function $\bar{F}(z, L)$. We could have used any independent set of polynomials for expanding the function. A proper error analysis including parameter correlations will always yield identical values for $\bar{F}(z_p, L)$ and its error. The final values for each energy are given in Table I,³⁴ and Fig. 1 shows the "best fit" polynomial, along with a rectangle indicating the magnitude of the experimental error at the position of the neutron exchange pole.

As an example, the values of η , the usual error $d\eta$, and the reduced chi square, χ^2/ν , as a function of L are shown in Fig. 2 for measurements at a deuteron lab energy of 45.3 MeV. As L increases, the data are reproduced to higher precision. The last major improvement occurs for $L=4$, where χ^2/ν falls below 1. Following the method of Refs. 10 and 11, the polynomial series is truncated at this point, and $\bar{F}(z_p, L)$ is converted into a value for η using Eq. (4).

As L increases, Fig. 2 shows that the error $d\eta$ increases exponentially, providing a strong motivation to choose L to be as small as possible. Between 5 and 56 MeV, only even values (either 2 or 4) have been chosen for L , since (as seen in Fig. 2, for 45.3 MeV) these values correspond to steps which produce a large improvement in χ^2/ν . In general, the errors decrease with increasing energy; however, a large increase in the decreasing trend occurs when L increases from 2 to 4 at 20 MeV.

The original extrapolation results for η produced values which seemed independent of the deuteron bombarding energy, and which were in good agreement with values of η obtained from two-nucleon models.^{35,18} However, it was pointed out by Santos and Colby²⁸ that the Coulomb penetrability P had to be included in these formulas. When this correction was made, the extracted value of η increased, particularly at low bombarding energies. The

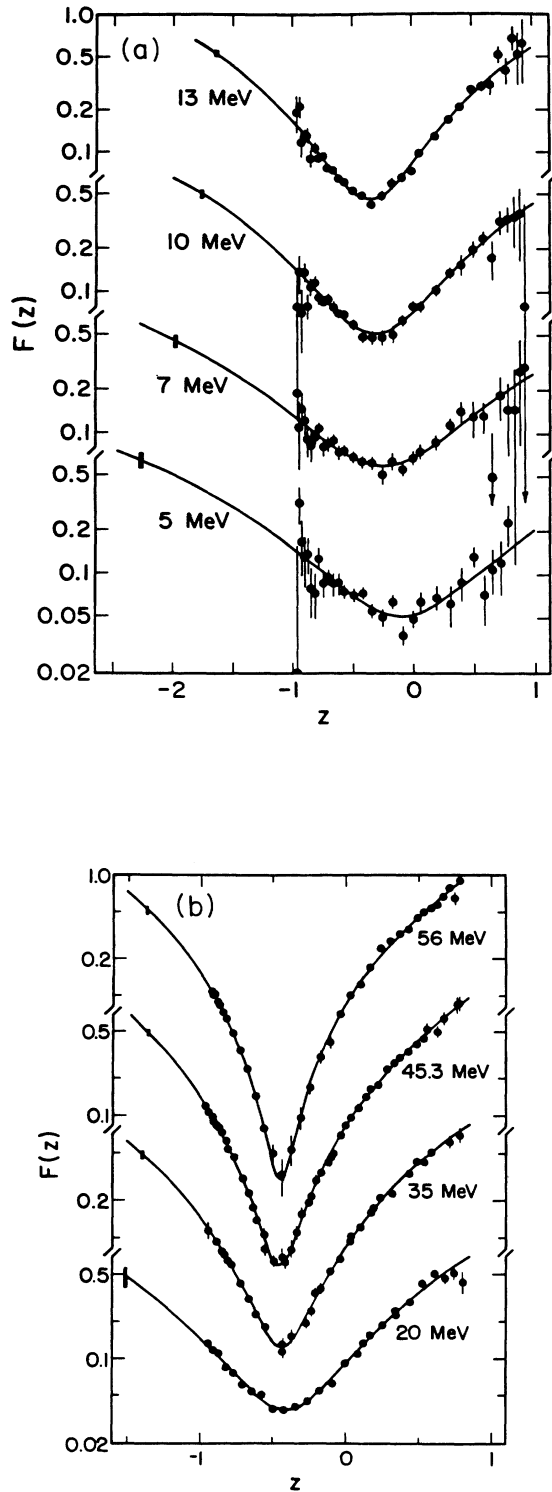


FIG. 1. Measurements of the extrapolation function $F(z)$ from the measurements of Refs. 10, 11, and 30. The smooth curves are the power series extrapolations discussed in the text. The rectangular points at $z < -1$ are centered on the values of the residue (their height spans the experimental error) determined by each extrapolation.

results are shown in Table I and Fig. 3, along with additional residues from Ref. 11 (open points) for which we do not have tabular angular distributions. Below 30 MeV these values are all substantially larger than the best theoretical value of η .

Especially small errors are often obtained by averaging together measurements at several energies. Without Coulomb penetrability corrections we obtain $\langle \eta \rangle = 0.0270 \pm 0.0005$ from our polynomial extrapolations (the contribution of each point to the average is weighted in accordance with its respective error). With the Coulomb correction, this average rises to $\langle \eta \rangle = 0.0293 \pm 0.0006$, a value inconsistent with the first average.^{36,37}

The errors which we quote with each average are clearly underestimates of the true errors. First, they neglect the truncation errors. In addition, each experimental point is treated independently without regard to possible systematic normalization or calibration problems which may be common to more than one measurement. This latter question will be treated briefly in Sec. VI.

Earlier in this section we stated that for a given order L , the quantity η and its experimental error were independent of the type of polynomial used to expand Eq. (3). This is true; however, the expansion coefficients a_l are usually highly correlated, even for Legendre polynomials. We can eliminate these correlations by expanding Eq. (3) in a set of polynomials orthonormalized over the data.³⁹

Such orthonormal polynomials Q_l are defined by the relation²⁶

$$\sum_i \frac{Q_l(z_i) Q_k(z_i)}{\Delta_i^2} = \delta_{lk}, \quad (6)$$

where the sum includes the set of data points, Δ_i represents the error in each point, and k spans the set of all polynomials of order up to l . If we now redefine the polynomial expansion in terms of the Q_l ,

$$F(z) = \sum_{l=0}^L a_l Q_l(z) + F_{tr}, \quad (7)$$

then the expansion coefficients are given by the measurements $F(z_i)$ as

$$a_l = \sum_i F(z_i) \frac{Q_l(z_i)}{\Delta_i^2}. \quad (8)$$

In this series expansion, the coefficients a_l are uncorrelated, and each has a statistical error of ± 1 .

We have stressed the potential importance of the truncation error, and the fact that this cannot be deduced from one set of measurements. We will find it useful to estimate these corrections with the use of a theoretical model for the polarization cross section amplitudes. Such a model will be reviewed briefly in the next section.

III. A MODEL FOR THE STUDY OF POLARIZED CROSS SECTION EXTRAPOLATION

A. Model amplitudes for $\vec{d} + p$ elastic scattering

In $\vec{d} + p$ elastic scattering, the most rapid z dependence of the observables will come from those amplitudes whose

TABLE I. Results of polynomial fitting with $F(z)$. Average $\langle \eta \rangle = 0.0293 \pm 0.0006$ (see text for explanation).

	Energy (MeV)							
	5	7	10	13	20	35	45.3	56
z_p	-2.252	-1.965	-1.751	-1.635	-1.500	-1.393	-1.361	-1.339
L	2	2	2	2	4	4	4	4
χ^2/ν	1.21	0.66	0.82	1.03	2.60	0.92	0.78	1.27
$\bar{F}(z_p, L)$	-0.623	-0.436	-0.486	-0.520	-0.477	-0.478	-0.486	-0.519
P	0.7781	0.8338	0.8791	0.9050	0.9367	0.9631	0.9713	0.9767
η	0.0433	0.0283	0.0299	0.0310	0.0275	0.0269	0.0270	0.0288
$d\eta$	0.0050	0.0028	0.0016	0.0010	0.0033	0.0020	0.0013	0.0015
	(0.0055)				(0.0053)			(0.0017)

singularities are nearest to the physical region ($-1 \leq z \leq 1$). If we want to study the convergence of a polynomial expansion in z of any physical observable, then it is crucial that we include the amplitudes associated with the nearest singularities. Our model contains the four amplitudes depicted schematically in Fig. 4; their location along the z axis is shown for a deuteron bombarding energy of 45.3 MeV. The specific form of the amplitudes in our model and formulae for the polarized cross section σT_{22} are given in Appendix A. In this section we will briefly outline the qualitative features of these amplitudes and their contribution to σT_{22} .

There are two components to the $d\eta$ vertices in the neutron exchange amplitude [see Fig. 4(b)], one from the deuteron S state and one from the D state. In our model

we represent this amplitude with the one-neutron-exchange Born term. Since the S -state term is much larger than the D -state term, the contribution to σT_{22} can be reliably calculated to first order in η . The effects of higher order terms in η will be significant only if all other sources of error are small ($\leq 2\%$).

The Rutherford amplitude [see Fig. 4(a)] has a pole at $z=1$. By itself, this amplitude for point charges makes no

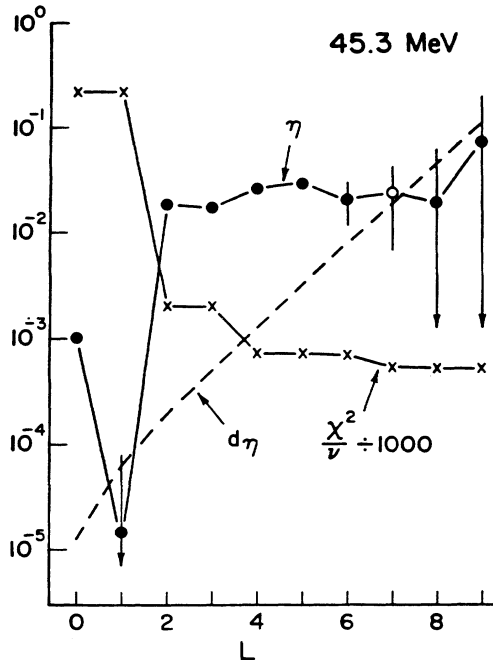


FIG. 2. Values of the residue η , its error $d\eta$, and the reduced chi square χ^2/ν of the fit for the 45.3 MeV data of Ref. 10 as a function of increasing L . (The open point at $L=7$ represents the magnitude of a negative value of η .)

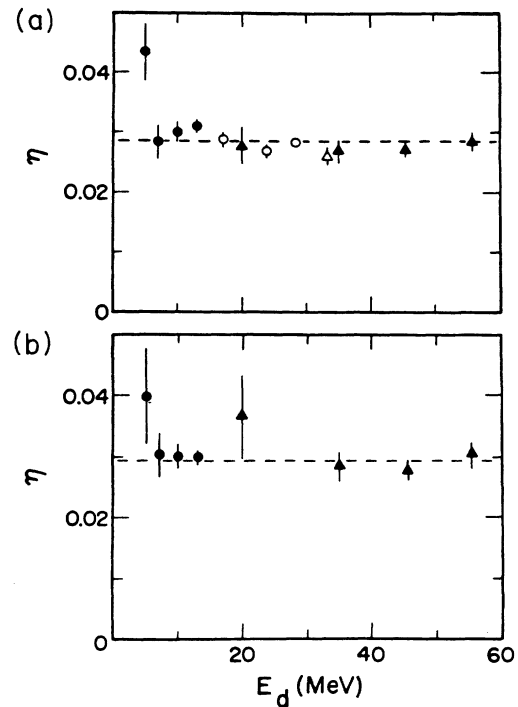


FIG. 3. (a) Values of η obtained by extrapolation using the function $F(x)$ of Eq. (2) after correction for the Coulomb penetrability. The extrapolation was truncated at $L=2$ (round points) or $L=4$ (triangular points). The open points are taken from Ref. 11, and solid points are values obtained in this work. (b) Values of η derived using a suppression factor [i.e., the function $G(z)$ of Eq. (10)], after correction for Coulomb penetrability. The extrapolation was truncated at $L=3$ (round points) or $L=5$ (triangular points). The average value is shown in both graphs as a dashed line.

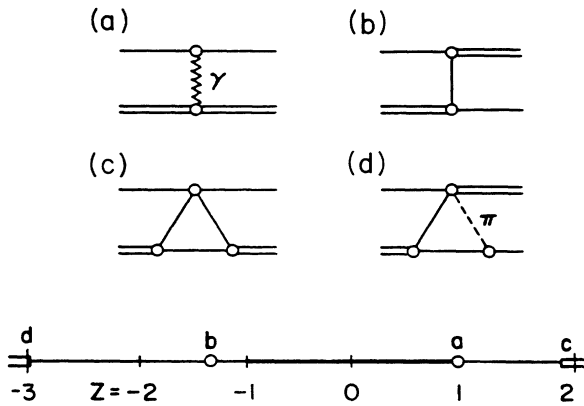


FIG. 4. Diagrams considered in the model for the z dependence of the polarized cross section. They are (a) Rutherford, (b) neutron exchange, (c) rescattering, and (d) pion triangle. The locations of the singularities (or branch cuts) for each amplitude along the z axis are shown at the bottom of the figure for a deuteron energy of 45.3 MeV (the neutron exchange singularity is shown here as a pole, rather than as a branch cut, for simplicity).

contribution to the tensor-polarized cross section; however, it does contribute through interference with other spin dependent amplitudes. Consequently, the extrapolation function $F(z)$ defined in Eq. (2) will be singular at $z=1$. This has consequences for any method which attempts to extrapolate the polarized cross sections to unphysical angles. The singularity at $z=1$ restricts the radius of convergence for any expansion of $F(z)$ to 1; for $|z| > 1$, the expansion is guaranteed to diverge. We will return in Sec. IV to methods for dealing with this problem in extrapolating to the neutron exchange pole.

The third term is the rescattering diagram shown in Fig. 4(c). This consists of a dpn vertex, scattering of a nucleon from the incident proton, and recombination of the two nucleons at a second dpn vertex. Our model incorporates the S - and D -state dpn vertices to first order in η , and we have used a simple N-N effective amplitude consisting of both a spin-independent and a spin-dependent term. In general, the rescattering amplitude is given by an integral involving the spectral function along the z -axis cut. For the S -state part, each vertex has been made pointlike, eliminating the integral. This is not adequate for the D state. In this case, the momentum dependence of the dpn vertex is taken from the Yamaguchi wave function, and the integration is done explicitly [see Eqs. (A15)–(A19)].

The last amplitude with a nearby singularity is the “pion” amplitude shown in Fig. 4(d). It represents virtual deuteron dissociation and a (highly) off-shell $NN \rightarrow \pi d$ amplitude followed by absorption of the virtual pion. In our model we are able to construct a reasonable estimate of the spin dependence of the Rutherford, neutron-exchange, and rescattering terms with amplitudes which have poles or cuts at the correct locations in z . For the “pion” amplitude, however, we have no reasonable model

of the spin dependence at low energies. However, the most important contribution to σT_{22} from this term is likely to occur through interference of the $l=0$ piece of this amplitude with the $l=2$ piece of the neutron-exchange Born term. We have chosen for our model a simple, spin-independent “pion” amplitude constructed from point form factors for every vertex.²¹ The expression for σT_{22} contains the interference term between this amplitude and the $l=2$ neutron exchange amplitude (with a free parameter for the overall strength).

All amplitudes which are not shown in Fig. 4 have singularities considerably farther from the physical region. The contribution of these terms to the polarized cross section is relatively slowly varying as a function of z . We approximated the effect of these distant singularities with two additional contributions to σT_{22} . The first contribution is a smooth background term, and the second is the interference of this background and the neutron-exchange Born term. Since the phase of the background amplitude relative to the preceding four amplitudes is not known, these two contributions are added incoherently to the polarized cross section with separate model coefficients.

The resulting model for the polarized cross section contains six free parameters representing the strength of various terms, one of which is the D -state normalization, η . While a more complicated form could have been used, it would be difficult for the experimental measurements to determine more than six free parameters. As can be seen from Table I, the polynomial expansions are able to fix between three and five parameters, depending on the deuteron energy.

The spin dependence of our model is oversimplified. Although this model is sufficient to reproduce observed σT_{22} angular distributions, it is not sufficiently general to make a simultaneous fit of all spin observables in this reaction. We could therefore remain skeptical of the quality of the results even though the values of η provided by this model seem reasonable. In Sec. V we perform a limited test of the model’s reliability by using parameters obtained from less precise measurements^{21,31} to predict the results of the more precise experiment²⁰ from Wisconsin.

B. Fitting procedure and convergence of the power series

For each angular distribution of σT_{22} , the six model parameters in Eq. (A23) were adjusted by the program MINUIT (Ref. 40) to minimize the chi square with respect to the data. At all energies a good representation of the measurements was obtained. An example of the data and the model fit at 45.3 MeV is shown in Fig. 5 and the final parameters for three representative energies are listed in Table II.⁴¹

The coefficient a for the effective N-N spin-independent term in the rescattering amplitude was very poorly determined by the data, as is evident from the very large errors shown in Table II. For the final parameter minimization we chose to fix it at a value of $a=30$. This is consistent with the results obtained by Locher and Mizutani,⁴² who used a simple model to fit $n + d$ elastic

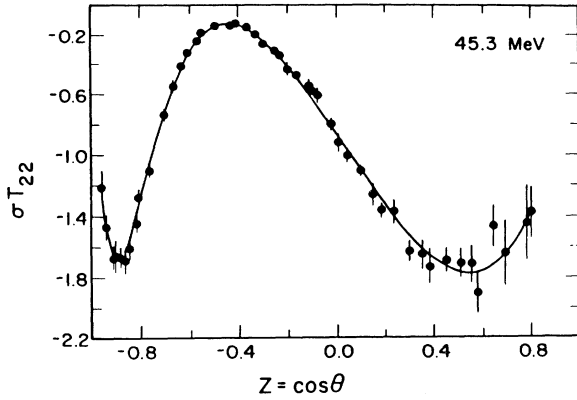


FIG. 5. Measurements of the tensor polarized cross section σT_{22} at 45.3 MeV. The smooth curve is the model fit to the data.

cross sections at low energies. The remaining parameters, given in Table III, exhibit a smooth variation with energy. Neither the value of η nor the χ^2/ν of the fit depend strongly on whether a is fixed or variable. Figure 6 shows the final values of η and their uncertainties at each energy.⁴³

Despite problems within individual angular distributions, the values of η form a consistent set, and the weighted average with Coulomb corrections is $\langle \eta \rangle = 0.0267 \pm 0.0009$. This value is several "standard deviations" from our extrapolated value $\langle \eta_{\text{ex}} \rangle = 0.0293 \pm 0.0006$. In part because there are more free parameters in our model than there are coefficients in the polynomial extrapolation, a larger error is obtained for the model determination of η . Our model value is close to that obtained from potential models of the deuteron.¹⁴

Since our model provides a high quality reproduction of the measurements of σT_{22} , we may use its functional form to investigate the convergence of the polynomial extrapolation. Using the model parameters fixed from experiment, we expanded the model amplitude in the orthonormalized polynomials of Eq. (6). Since the model amplitude can be calculated to any order in l , we can examine the convergence properties of the resulting polynomial expansion. We define $\tilde{F}(z, L)$ to be the polynomial approximation of order L to our model function:

$$\tilde{F}(z, L) = \sum_{l=0}^L \tilde{a}_l Q_l(z), \quad (9)$$

TABLE II. Initial results of model minimization.

	Energy (MeV)		
	20	35	45.3
η	0.0250 ± 0.0019	0.0260 ± 0.0014	0.0259 ± 0.0009
a	70 ± 60	30 ± 50	16 ± 25
b	-2.7 ± 8.2	-2.7 ± 4.8	-2.3 ± 1.2
c	-3.59 ± 0.82	-3.67 ± 0.67	-3.84 ± 0.64
d	0.020 ± 0.002	0.020 ± 0.007	0.020 ± 0.003
e	0.52 ± 0.41	0.49 ± 0.28	0.63 ± 0.28
χ^2/ν	2.95	1.05	0.89

where the \tilde{a}_l in Eq. (9) are the model expansion coefficients. If we extrapolate this truncated expansion to the neutron exchange pole, z_p , then plotting $\tilde{F}(z_p, L)$ as a function of L will demonstrate the convergence properties of our model.

In Fig. 7 we plot the quantity $-0.0541\tilde{F}(z_p, L)$ as a function of L (solid circles), for deuteron energies of 20 and 45.3 MeV. From Eq. (4) this should equal $\bar{\eta} \equiv P\eta$. For each energy the function does not converge at large L , but continues to oscillate about the value determined by the minimization. This problem is quickly traced to the presence of the Rutherford amplitude in the model cross section. There is no convergence at the exchange pole because the radius of convergence is bounded by the Rutherford singularity at $z=1$.

IV. REMOVAL OF THE RUTHERFORD SINGULARITY AND TRUNCATION ERRORS

As we saw from Sec. III, the Rutherford singularity at $z=1$ prevented us from extrapolating to the neutron exchange pole. Methods for dealing with the Rutherford singularity are well known. One can

- (1) suppress the singularity by multiplying the extrapolation function by an appropriate suppression factor;¹⁹
- (2) use conformal mapping to map the Rutherford singularity away from the physical region, so that one can extrapolate the mapped function to the neutron exchange pole;^{44,26}

or, one can use both methods (1) and (2) together.

In the process we will compare the measurements with the extrapolations based on substituting model values for the original measurements. This will provide us with information on the truncation errors, and we will see why the original extrapolation procedure produced answers close to the theoretical values.

A. Suppression of the Rutherford singularity

Using method (1), we have removed the nonlogarithmic part of the Rutherford singularity by defining a new extrapolation function $G(z)$ through¹⁹

$$G(z) = p^2 \sigma T_{22} \frac{(z - z_p)^2 (1 - z)}{(1 - z^2)(1 - z_p)}. \quad (10)$$

The new function $G(z)$ has the same value at the exchange pole as $F(z)$. In Fig. 8 we show the data for $G(z)$ as a function of z . The solid curves are the best fit polynomials we used for extrapolation. The solid rectangle at $z < -1$ gives the position of the neutron exchange singularity, and marks the extrapolated value $\bar{G}(z_p, L)$ and its error at this point.

In Table IV we give the results of the power series fit to the new function $G(z)$. At energies where the reduced chi square is greater than 1, the error in parentheses includes the additional effects of chi square. The values of η are corrected for the Coulomb penetrability. Because of the new $1-z$ factor in the numerator of Eq. (10), the op-

TABLE III. Final results of model minimization. Average $\langle \eta \rangle = 0.0267 \pm 0.0009$ (see text for explanation).

	Energy (MeV)							
	5	7	10	13	20	35	45.3	56
η	0.0280	0.0300	0.0298	0.0307	0.0249	0.0260	0.0259	0.0276
$d\eta$	0.0200	0.0060	0.0050	0.0030	0.0025	0.0019	0.0014	0.0022
a	30	30	30	30	30	30	30	30
b	-15	-0.32	-4.4	-6.5	-4.7	-2.75	-2.2	-1.1
c	-4.0	-4.7	-2.8	-5.0	-3.7	-3.7	-3.7	-2.4
d	0.022	0.025	0.015	0.027	0.020	0.020	0.020	0.013
e	0.2	0.3	0.1	0.4	0.3	0.5	0.6	0.3
χ^2/ν	1.37	0.87	1.01	1.06	2.87	1.00	0.87	1.52

timum value of L increases by one unit over the corresponding value of L needed with the function $F(z)$. In Fig. 3(b) we show a graph of the values and errors for η using the function $G(z)$. Except for the value at 20 MeV, the determined values of η are remarkably similar in the two cases shown in Fig. 3. This may be related to the similar choice of L values for the power series extrapolations at each energy.

The new average value of η is $\langle \eta \rangle = 0.0296 \pm 0.0006$, a value close to that obtained with $F(z)$. The new function does, however, give results more consistent with energy. The χ^2/ν for the average $\langle \eta \rangle$ is 0.29 with $G(z)$, as compared to 2.06 for $F(z)$. This is, in part, a result of the uniformly larger errors obtained with $G(z)$, which required one additional polynomial coefficient in the fitting process.

In order to show the convergence properties of the new extrapolation function, we have calculated $G(z)$ with our

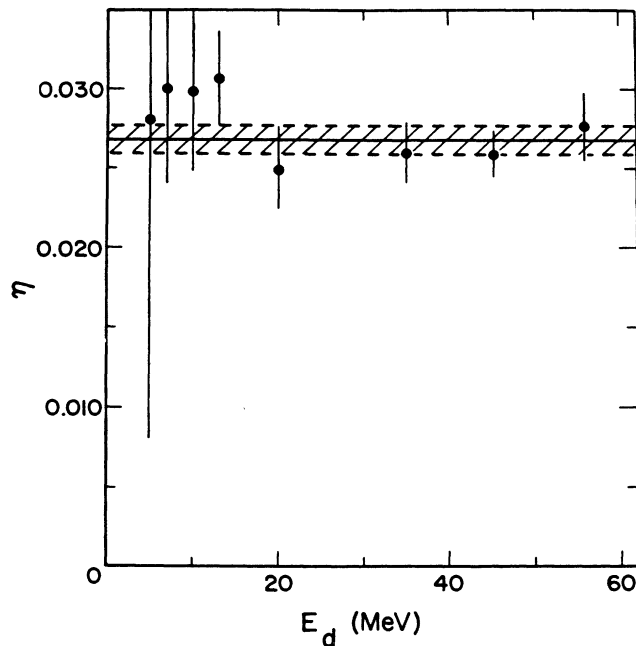


FIG. 6. Values of η obtained from our model at eight energies. The solid line and the shaded region are the weighted average and its error.

model and expanded that function in orthonormal polynomials, as we had done previously with $F(z)$. If we truncate the polynomial expansion of the model at order L , this gives us a function $\tilde{G}(z, L)$. The open circles in Fig. 7 show $-0.0541\tilde{G}(z_p, L)$ as a function of L . The convergence of $\tilde{G}(z, L)$ with L is dramatically improved. At both 20 and 45.3 MeV, $\tilde{G}(z, L)$ has converged to within 1% of the model value of η for $L \geq 6$.

From Fig. 7 we see that, for the original extrapolation of $F(z)$, the values deduced for η (the solid rectangles in Fig. 7) are actually quite close to the final values obtained using the convergent function G . However, by observing the oscillations as a function of L , we see that these results were really quite fortuitous: it just happened that

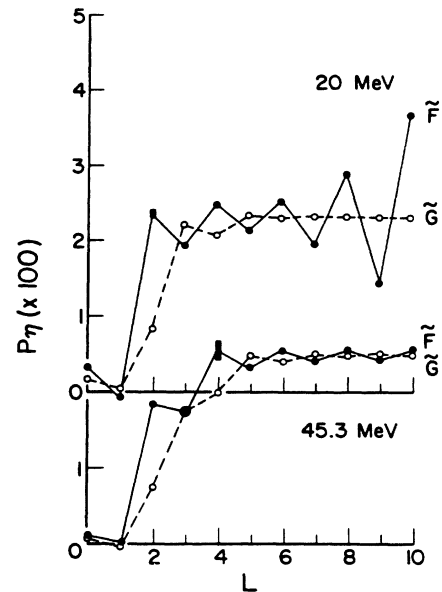


FIG. 7. Values of the residue $P\eta$ as a function of L , the maximum order of the extrapolating polynomial. The solid circles are taken from our model of the extrapolation function $\tilde{F}(z, L)$ of Eq. (9). The rectangular points are the points chosen in the analysis of Refs. 10 and 11; the height of the rectangle represents the quoted experimental error. The open circles are taken from our model for the function $\tilde{G}(z, L)$ defined in the text.

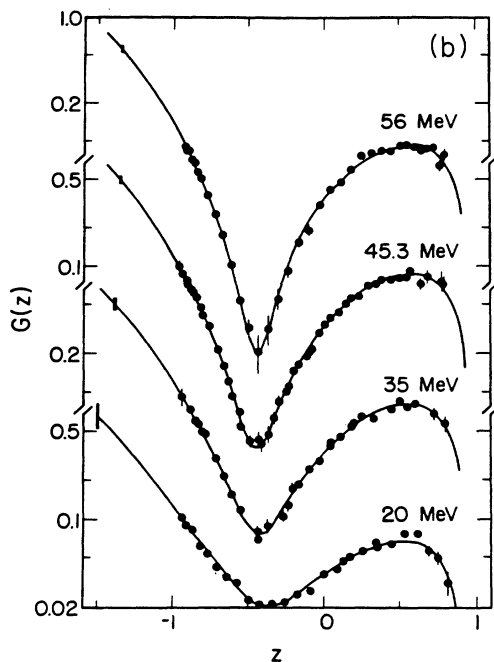
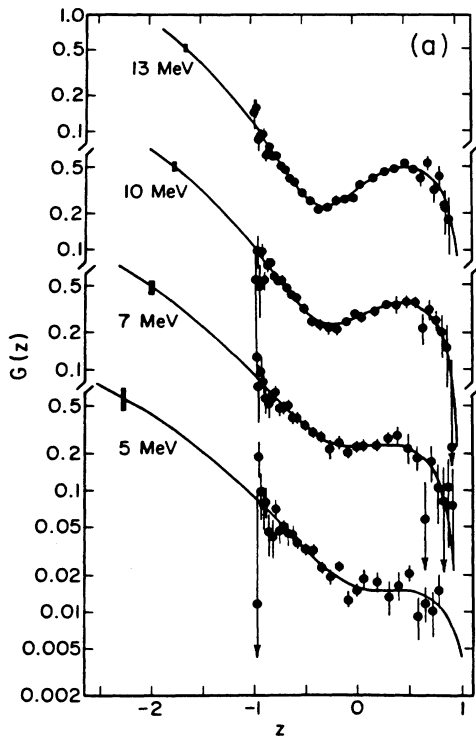


FIG. 8. Measurements of the extrapolation function $G(z)$ from Refs. 10, 11, and 30. The smooth curves are the power series extrapolations discussed in the text. The rectangular points at $z < -1$ indicate the values of the residue and its error for each extrapolation.

the data produced a value of L where the extrapolation function F coincided with a “good” value for η . Thus, the confidence which arose due to the agreement between the theoretical and extrapolated values of η was misplaced.

The truncation error arises from higher-order terms which cannot be inferred from a measurement of the polarized cross sections. With a single set of measurements, the precision of the data sets a limit on L , and we have no direct way of estimating the truncation error. We will investigate two possible methods for estimating this error.

The first involves subsequent measurements of data at the same energy, but with significantly greater precision. This will allow us to calculate higher-order terms in a polynomial expansion of the data. In this way we can experimentally check the convergence of the polynomial series. Although there will always remain a truncation error, we would be reassured if we could see that successive terms in a polynomial expansion contributed less and less to the final answer.

The second method estimates the size of the higher-order terms and the truncation error from our model. Such a procedure is model dependent. The high-precision measurements from Casavant *et al.* at Wisconsin²⁰ allow us to check both of these methods. We will discuss this in detail in Sec. V.

B. Conformal mapping of the data

A second technique to ensure convergence of a polynomial expansion is to apply a conformal mapping in the angle variable z before expanding the data. Conformal mapping techniques have two advantages. First, they can increase the radius of convergence of a polynomial expansion. Second, they can speed up the rate of convergence. For these reasons, conformal mapping techniques can be powerful tools even for inelastic reactions where no Rutherford singularity is present.⁴⁵

In this context the optimal conformal mapping technique introduced by Cutkosky and Deo⁴⁴ offers an extremely useful method for expanding any set of data. If we have a function which is analytic between the points z_1 and z_2 , then the optimal conformal mapping technique guarantees that the function expanded in the mapped variable will converge faster than any other expansion in the region $z_1 \leq z \leq z_2$ (hence this particular conformal mapping is “optimal”). Since this method is so important to the extrapolation problem, we will consider it in detail.

For the moment, we will neglect the effects of Coulomb distortions on the neutron exchange singularity and return to them later in this section. In this case the extrapolation function $F(z)$ is regular at the pole position z_p . To implement the Cutkosky-Deo procedure, we perform three transformations of the variable z . First, we use a linear transformation to map the region containing the data onto the interval $(-1, 1)$, as suggested in Ref. 19. Next, we perform a transformation which symmetrizes the location of the two nearest singularities of $F(z)$ about $z=0$. The closest singularities of $F(z)$ are the Rutherford singularity (originally at $z=1$, but located at $z > 1$ following the first transformation), and the “pion” singularity at $z < -1$.

TABLE IV. Results of polynomial fitting with a suppression factor. Average $\langle \eta \rangle = 0.0296 \pm 0.0008$.

	Energy (MeV)							
	5	7	10	13	20	35	45.3	56
L	3	3	3	3	5	5	5	5
χ^2/ν	1.25	0.65	0.84	0.98	2.24	0.91	0.79	1.24
η	0.0398	0.0303	0.0300	0.0298	0.0363	0.0286	0.0277	0.0305
$d\eta$	0.0080 (0.0088)	0.0036	0.0020	0.0013	0.0043 (0.0064)	0.0026	0.0017	0.0019 (0.0021)

Finally, the symmetrized plane is mapped onto a unifocal ellipse using the iterative approximation scheme described in Ref. 44. The last two steps of this procedure leave the endpoints of the data region (at $z = \pm 1$) unchanged. The Rutherford singularity has thus been mapped away from the “physical” region, and the neutron exchange point is left within the resulting convergence ellipse. In Fig. 9 we show the data points and the position of the neutron exchange pole following the conformal mapping. In Table V we list the position of the neutron-exchange pole before and after mapping, and the position of the “pion” pole before mapping.

In order to determine the effects of conformal mapping, we recalculated the orthogonal polynomials defined in Eq. (6),

$$\sum_i \frac{Q_i(z_i^m) Q_k(z_i^m)}{\Delta_i^2} = \delta_{ik}, \quad (11)$$

using the mapped angle variable z^m . Then we repeated the polynomial expansion of the data,

$$\bar{F}^m(z^m, L) = \sum_{i=0}^L a_i^m Q_i^m(z^m), \quad (12)$$

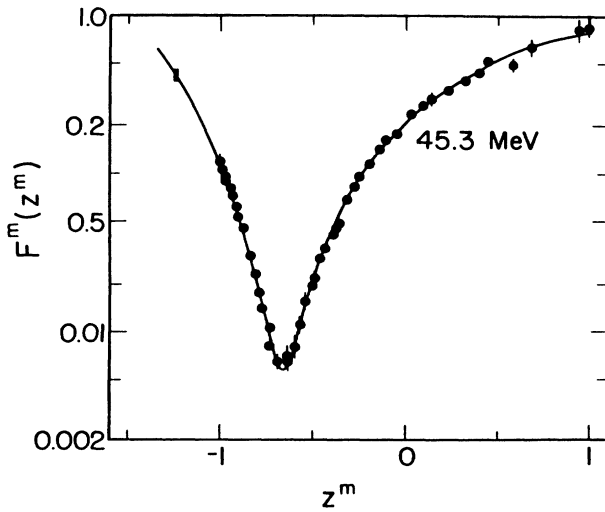


FIG. 9. Values of the conformally mapped extrapolation function $F^m(z^m)$ at 45.3 MeV. The smooth curve shows the best power series extrapolation. The rectangular point at $z < -1$ denotes the value of the residue and its error as determined by extrapolation in the conformally mapped variable.

and of the model,

$$\tilde{F}^m(z^m, L) = \sum_{l=0}^L \tilde{a}_l^m Q_l^m(z^m), \quad (13)$$

and we extrapolated each expansion to the exchange pole. In Fig. 9 the solid curve shows the best polynomial reproduction of the mapped data at 45.3 MeV obtained using $L=5$.

We can now compare results of conformal mapping with those obtained with a suppression factor. The mapped values of η and their errors are listed in Table VI, and shown as the solid dots in Fig. 10. Values obtained with a suppression factor (listed in Table IV) are shown as the open circles in Fig. 10 for comparison. Corrections have been made for Coulomb penetrability. Both mapping and suppression require the same value of L . The mapped values are consistently about 20% lower, as shown by the average $\langle \eta \rangle = 0.0244 \pm 0.0006$ for mapping compared to $\langle \eta \rangle = 0.0296 \pm 0.0008$ with a suppression factor.

First, we see that the experimental errors are far smaller than the true uncertainty. Two essentially equivalent methods for determining η give results which differ by about seven “standard deviations”; these vastly different results are inferred from the same data set! Unless one of the methods is poorly founded, the small error estimates obtained from polynomial extrapolation are clearly unreliable.

We can obtain estimates of the truncation error in each procedure from our model. When we expand our model amplitudes in the orthonormal polynomials from Eq. (6), the lower partial waves are constrained by the data. We have examined model extrapolation using a suppression

TABLE V. Location of singularities (before and after conformal mapping).

Energy (MeV)	z_p	z_p^m	z_π
56	-1.34	-1.28	-2.64
45.3	-1.36	-1.24	-2.98
35	-1.39	-1.26	-3.49
20	-1.50	-1.26	-5.16
13	-1.64	-1.20	-7.27
10	-1.75	-1.22	-9.08
7	-1.96	-1.25	-12.43
5	-2.25	-1.46	-16.90

TABLE VI. Results of polynomial fitting with conformal mapping. Average $\langle \eta \rangle = 0.0244 \pm 0.0006$.

	Energy (MeV)							
	5	7	10	13	20	35	45.3	56
L	3	4	4	4	5	5	5	5
χ^2/ν	1.26	0.56	0.85	1.02	2.32	0.98	0.99	1.49
η	0.0239	0.0252	0.0277	0.0244	0.0254	0.0244	0.0237	0.0269
$d\eta$	0.0036 (0.0040)	0.0033	0.0020	0.0014	0.0016 (0.0024)	0.0013	0.0010	0.0013 (0.0016)

factor and conformal mapping. The model results (the open circles in Fig. 7 and the open squares in Fig. 11) smoothly approach the asymptotic values for η ; for any L the truncation correction is the difference between the value in our model, and the value of η obtained by truncating at L . These corrections are listed in Table VII. For all cases considered, our model with adjusted parameters provides a good description of the data, as well as the various extrapolated versions of it. Thus if we apply a "truncation correction" derived from our model to any extrapolated value, we will always obtain the same answer: the model value. Thus, the differences among extrapolation techniques, such as those shown in Fig. 10, can be attributed entirely to the effects of truncation.

Borbély *et al.*²⁴ have used comparisons such as that in Fig. 10 in situations where the difference between the two methods is small, and they argue that the underlying truncation errors must be negligible. This method may not be effective, as there is no assurance that any set of methods will bracket the correct value.

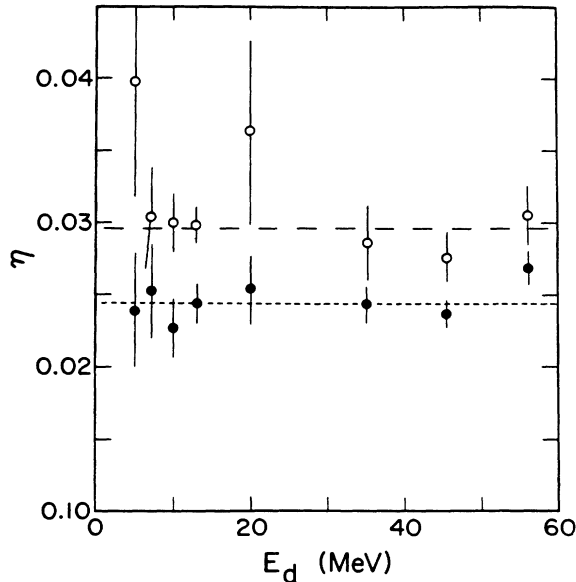


FIG. 10. Values of η obtained by extrapolation at eight energies. The solid circles are obtained using the conformally mapped function $F^m(z^m)$ of Eq. (11). The open circles are the values obtained using the suppression factor of Eq. (10). The long- and short-dashed lines show the average $\langle \eta \rangle$ using suppression factor or conformal mapping, respectively.

In our introduction to conformal mapping, we neglected the Coulomb distortion effects at the neutron exchange singularity. Inclusion of these effects has serious consequences for our choice of mapping function. In Fig. 12(a) we show the Coulomb distortions for the $\bar{d} + p$ neutron exchange amplitude. These effects convert the neutron exchange pole into a cut which begins at the pole position z_p .⁴⁶ In Fig. 12(b) we show the singularity structure for $F(z)$ at 45.3 MeV when this cut is included. In our conformal mapping procedure, we used the "pion" singularity as the boundary of our ellipse; therefore, the mapped function $F(z)$ is not analytic inside the ellipse. The theorems of Cutkosky and Deo⁴⁴ require the mapped function to be analytic inside the convergence region. Since our extrapolation function violates this condition, the theorems which prove optimal convergence do not apply; therefore we have no guarantee that the conformal mapping procedure will give the fastest convergence of a polynomial expansion. Note that the same problem arises as well for inelastic reactions like ${}^2\text{H}(d,p){}^3\text{H}$.

In the final analysis, the "optimal conformal mapping" technique is also plagued by ambiguity. Like the original extrapolation problem, the truncation errors cannot be measured for any one set of data. Coulomb distortions

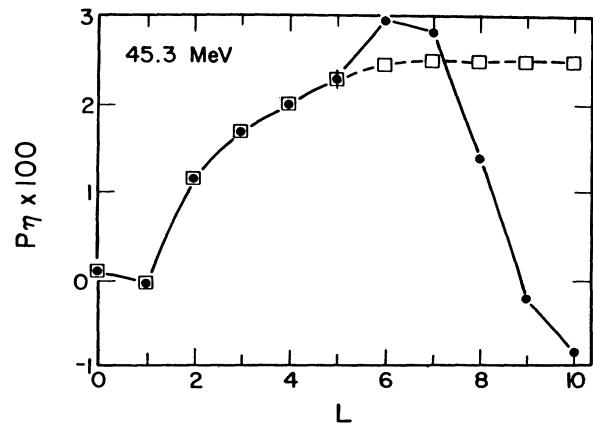


FIG. 11. Dependence of η on L for conformally mapped extrapolation. The solid circles give values of η determined from the polynomial extrapolation of Eq. (11). The open squares give values of η obtained by extrapolating our model. The solid circle with an error bar denotes the best polynomial value and its experimental error.

TABLE VII. Truncation corrections.

	Energy (MeV)							
	5	7	10	13	20	35	45.3	56
$F(z)$	-0.0153	-0.0017	-0.0001	-0.0003	-0.0026	-0.0009	-0.0011	-0.0013
$G(z)$	-0.0118	-0.0003	-0.0002	0.0009	-0.0114	-0.0026	-0.0018	-0.0031
$F^m(z^m)$	0.0041	0.0048	0.0071	0.0063	0.0005	0.0016	0.0022	0.0006

convert the neutron exchange pole into a cut. If we extrapolate the function $F(z)$ to this point, we are extrapolating to an “incompletely removed” singularity, a risky procedure.

V. EXPERIMENTAL VERIFICATION OF LARGE TRUNCATION ERRORS

In Sec. IV we suggested that truncation errors were likely to be considerably larger than the experimental errors. At that point we were using model calculations for the polarized cross sections. Clearly, our results depended on the reliability of our model. In order to evaluate our claims, it would be useful to have independent measurements of the tensor-polarized cross sections, taken at an energy where a set of data already existed, and more precise than the previous data. With such data we would be able to check whether our model correctly predicted higher-order terms, and from that estimate the quality of the truncation corrections.

We have found the data of Casavant *et al.*,²⁰ taken at Wisconsin, to be extremely useful in this regard. The authors have measured polarized $\bar{d} + p$ scattering for 10 MeV deuterons, an energy previously measured by Gruebler *et al.*¹¹ The Wisconsin group achieved an experimental precision five times better than previously obtained, allowing them to obtain two more terms in a polynomial extrapolation. One can then ask the following questions:

(1) How large is the contribution associated with these two additional terms, relative to the experimental error obtained by Gruebler?

(2) Is the extrapolated value for η converging rapidly, so that higher-order terms become progressively smaller as the order L increases?

(3) How useful was our model for the polarized cross sections? If we fit our model to the Gruebler polarized cross sections, will it correctly predict the contributions from higher-order terms?

We have determined η from the Wisconsin measurements using “optimal” conformal mapping techniques. The results are shown in Table VIII, where they are compared with η from the data of Gruebler *et al.* at the same energy. The Wisconsin data are sufficiently precise that we may calculate two more terms in the polynomial expansion.

These two determinations of η at 10 MeV differ substantially. Using the data of Gruebler *et al.* we obtained a value for η of 0.0227 ± 0.0020 , while the Wisconsin data gave a value of 0.0284 ± 0.0011 . Note that the new value of η is almost three “standard deviations” away from the old value (using the standard deviation from Ref. 11). Therefore, the experimental errors are unreliable indicators of the precision with which we can determine η .

In Ref. 20 Casavant *et al.* saw no sign of convergence for the standard extrapolation technique. As shown in Sec. IV, this is due in part to the presence of the Rutherford singularity at $z=1$. The same extrapolation is shown in Fig. 13, this time with the Rutherford singularity removed through conformal mapping. Past $L=3$, the values steadily decline, suggesting a trend towards convergence.

Figure 13 also includes the terms suggested by our model, whose parameters were determined from the less precise measurements of Ref. 11. The model predictions for $L=5$ and 6 are within the errors given by the Casavant measurements, thus indicating that the model may be reliably used to estimate additional extrapolation terms and the resulting truncation corrections. To obtain results with the presently quoted “experimental errors,” our model suggests that at least three additional terms must be measured experimentally. This would require a reduction of an order of magnitude in the size of the experimental errors, which is not presently feasible.

Two other theoretical model studies have estimated the size of the truncation corrections. Locher and Mizutani²¹ used a simple model for $n + d$ scattering, and estimated that truncation corrections could be as large as 15% for angle-extrapolation procedures. Berthold and Zankel²² solved the Faddeev equations for $n + d$ scattering N-N potentials with a known value for η . They then extrapolated σT_{22} to the proton exchange pole using polynomials fitted to a set of calculated points. They found that the extrapolated value typically differed from the input value

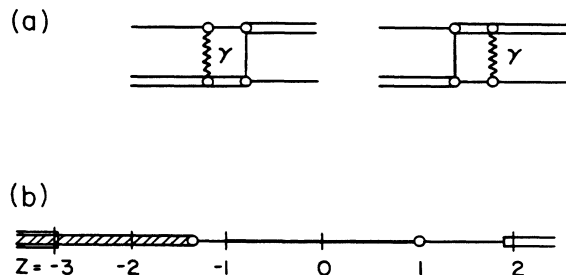


FIG. 12. (a) Diagram of the Coulomb distortion effect on the neutron-exchange amplitude for $d + p$ elastic scattering. These Coulomb effects convert the neutron-exchange “pole” of Fig. 4(b) into a cut. (b) Singularity structure of the function $F(z)$ of Eq. (2) when the neutron exchange singularity is converted into a cut (the location of singularities is appropriate for a deuteron energy of 45.3 MeV).

TABLE VIII. Comparison of extrapolation and the method of asymptotical coefficients.

Energy (MeV)	Extrapolation			MAC	
	η	L	χ^2/ν	η	L
56	0.0269 ± 0.0013	5	1.49	0.0248 ± 0.0017	5
45.3	0.0237 ± 0.0010	5	0.99	0.0225 ± 0.0013	5
35	0.0244 ± 0.0013	5	0.98	0.0242 ± 0.0018	5
20	0.0254 ± 0.0016	5	2.32	0.0266 ± 0.0025	5
10 (Grüebler)	0.0227 ± 0.0020	4	0.88	0.0257 ± 0.0037	4
10 (Casavant)	0.0284 ± 0.0011	6	1.16	0.0295 ± 0.0020	6
Average	$\langle \eta \rangle = 0.0255 \pm 0.0005$			$\langle \eta \rangle = 0.0248 \pm 0.0008$	

of η by several percent. The best agreement was obtained with the Graz-II N-N potential. The difference between “true” and “extrapolated” values for η were 5.25% and 5.62% for neutron lab energies of 5 and 10 MeV. This is comparable to the present experimental errors at these energies. Other N-N potentials produced even larger differences. Both of these works support our qualitative conclusions that the truncation errors are likely to be several times larger than the experimental errors.

VI. SYSTEMATIC EXPERIMENTAL ERRORS IN THE POLARIZED CROSS SECTION

The experiments for deuteron-proton elastic scattering are subject to systematic errors besides those arising from the statistical angular distribution errors considered in the analysis of Ref. 8. The cross section usually carries a normalization error of at least 3%. The calibration of the beam polarization is based on a bootstrap method brought up from lower energy, and is expected to be accurate to roughly 3% as well.⁴⁷

However, even such general careful estimates have clearly overlooked problems in the agreement between

measurements from different experimental groups. A comparison of the T_{22} measurements of Refs. 10 and 11, as shown in Ref. 48, gives differences in the measurements at the largest values of T_{22} of about 15%. Similar discrepancies exist between the measurements at 33 MeV from Ref. 11 and at 35 MeV from Ref. 10. Yet both groups extract essentially the same value of η at these energies! A closer examination of the two sets of data reveals that both magnitude and zero shifts are present. The extrapolation function matters most where it is large. At those angles, the experimental differences happen to be small and the values for σT_{22} are coincidentally the same.⁴⁹ (The cross sections agree very well.)

The beam polarizations at the higher energies were determined from $\bar{d} + {}^4\text{He}$ elastic scattering where the analyzing powers are very large. Comparing the measurements of the groups from Berkeley⁴⁷ and SIN⁵⁰ reveals that, for this calibration experiment, results differ at all energies and in ways that are not systematic with energy, angle, or observable. Thus there are problems not only with the beam polarization, but also with the extraction of the polarized cross sections from the experimental measurements. Again, both scale factor and zero shifts appear to be involved. The calibration used at SIN gives the larger value of T_{22} at 45 MeV.⁴⁸ This calibration has been used as the basis for the Osaka measurements³⁰ at 56 MeV. The extrapolated value of η at 56 MeV thus appears somewhat higher in all of our analyses, just as the 35 and 45.3 MeV points from Berkeley appear low. It is clear that systematic experimental errors considerably exceed the statistical precision of the $\bar{d} + p$ data, especially at the higher energies, and now constitute yet another limitation in the reliability of η taken from $\bar{d} + p$ angular extrapolations. Before any further conclusions can be drawn regarding the precision of the angular extrapolation technique by comparisons with the theoretical values of η , these experimental differences must be resolved.

VII. CONCLUSIONS

At first glance, extrapolation of cross sections for polarized $\bar{d} + p$ elastic scattering [or the ${}^2\text{H}(d,p){}^3\text{H}$ reaction] appears to give a very precise direct determination of η with small errors. However, closer examination reveals that this procedure contains a number of hidden sources of error which we have attempted to delineate in this paper. The earliest attempts to determine η neglected

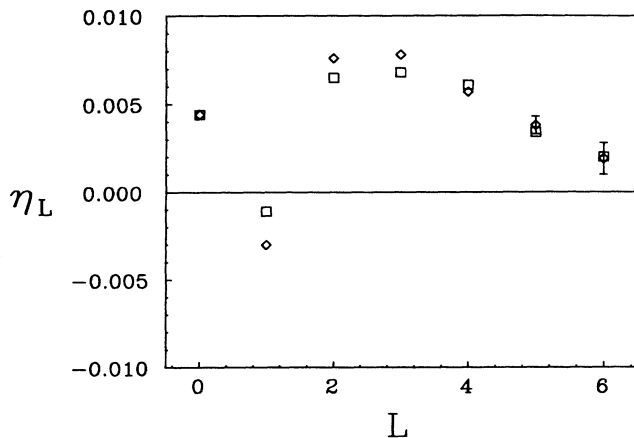


FIG. 13. Values of η vs L for the high-precision Wisconsin data of Ref. 20 (diamonds with error bars), and values from our model in which the parameters were determined from the less precise data of Ref. 11 (squares).

Coulomb penetrability effects and truncation corrections, both of which are relatively large. In more recent measurements, the truncation corrections are neglected, leading to quoted errors which are far smaller than the "true" uncertainties in this procedure.

In order to demonstrate the size of the uncertainties in this process, we have used several different methods. First, we showed that different procedures for extrapolation (conformal mapping and singularity suppression) gave very different values for η . Second, we showed that a theoretical model for the $\vec{d} + p$ amplitude predicts large truncation errors in the extrapolation procedures. Finally, we show that recent high-precision data for $\vec{d} + p$ scattering allows us to "measure" some of the truncation error from previous experiments. These experimental corrections are large and in quantitative agreement with the predictions from our theoretical model.

Another vexing problem for systematic error estimates is found in the disagreement among various experimental groups regarding $\vec{d} + p$ analyzing powers. These discrepancies have complex origins, and the close agreement in values of η quoted from independent sets of measurements tended to provide a false sense of confidence in the consistency of the data. Until these differences are resolved, no precise value of η from these experiments can be regarded as credible. Both the values of the beam polarization and the extraction of analyzing powers from count rates need to be addressed. Such an enterprise would be considerably easier if a primary standard for intermediate energy deuteron beam polarization was available.⁵¹

Progress in determining η from extrapolation will probably come only by simultaneously investigating the errors by several methods. The high-precision Wisconsin data²⁰ at 10 MeV gave a direct measure of the truncation error in previous experiments. These data show a slow trend toward convergence, although we suggest that even more precise data will be necessary before truncation errors can be neglected. Theoretical models for the polarized amplitudes are very useful in suggesting the magnitudes of the truncation errors.

We believe that the present uncertainties in η from extrapolation are at least as large as 10%, due to uncertainties in the data and to large truncation errors. This is certainly true in the $\vec{d} + p$ data which we have analyzed at

length; similar corrections are likely to be present in the ${}^2\text{H}(\text{d},\text{p}){}^3\text{H}$ reaction data. At this level of uncertainty, angular extrapolation does not compare favorably with the direct determination of η from sub-Coulomb stripping reactions,^{5,6} nor with the indirect determination of η through the close connection between η and Q (the deuteron quadrupole moment).¹⁴

ACKNOWLEDGMENTS

The authors would like to thank Prof. W. Gruebler for allowing us to use some of the ETH-Zürich T_{22} data for our analyses, and for spirited discussions regarding comparisons of data and extrapolation methods. We also thank Prof. H. E. Conzett for allowing us to use the Berkeley T_{22} data and Prof. K. Hatanaka for allowing us to use the Osaka T_{22} data for our analyses. One of the authors (J.T.L.) would like to acknowledge conversations with R. Amado, T. E. O. Ericson, and M. Locher regarding both extrapolation methods and the importance of the quantity η . Another of the authors (E.J.S.) would like to acknowledge conversations with P. Colby and H. E. Conzett on problems associated with extrapolation techniques. This research was supported in part by the U.S. National Science Foundation.

APPENDIX A: MODEL FOR THE POLARIZED CROSS SECTION

As we discussed in Sec. III, our model includes a parametrization of the diagrams for $\vec{d} + p$ scattering with the closest singularities to the physical region. The four diagrams discussed here are shown in Fig. 4, along with the locations of their singularities on the z axis for 45.3 MeV deuteron bombarding energy. These diagrams include the Rutherford amplitude, neutron-exchange term, nucleon-nucleon rescattering term, and a "pion" term. In addition, we include a smooth background to represent the effect of all other more distant singularities. This appendix summarizes the amplitudes in our model.

The polarized cross section can be conveniently expressed in terms of the helicity representation⁵² for the scattering amplitudes. With m and M being the helicities of the proton and deuteron, respectively (primed in the outgoing channel), we obtain

$$\sigma T_{k\nu} = \sigma_{k\nu} = \frac{\sqrt{3}}{6} (2k+1)^{1/2} \sum_{M_1 M_2 m m' M'} (-1)^{1+M_2+\nu} \begin{pmatrix} 1 & 1 & k \\ M_1 & -M_2 & \nu \end{pmatrix} t_{m'M'M_2}^*(\theta, E) t_{m'M'm_1}(\theta, E), \quad (\text{A1})$$

where t , the scattering amplitude, is a function of the scattering angle and energy. As a first approximation, the scattering amplitude is expressed as the sum of four terms,

$$t = t_C + t_X + t_{\Delta S} + t_{\Delta D}, \quad (\text{A2})$$

where the quantum number indices have been suppressed and the specific amplitudes refer to the Rutherford, neutron-exchange, and the S - and D -state parts of the re-

scattering diagram. It was felt that enough was known about these diagrams so that their relative phases could be included explicitly. The z dependence of the pion exchange term and the background were assumed to carry unknown phases, and these terms were added incoherently when the contribution to the polarized cross section from Eq. (A2) was calculated.

The tensor character of the polarized cross section demands that each term in the expression for the polar-

ized cross section contain at least one $l=2$ component. Assuming that the asymptotic D - to S -state ratio, η , is small, we kept only the first order terms in the $l=2$ component. Thus, only terms linear in η were retained. This allowed us to make a considerable reduction in the number of terms present and in the recoupling algebra associated with each one. Since interference terms can occur within the amplitude given in Eq. (A2), both $l=0$ and 2 pieces of the individual amplitudes were initially calculated.

The amplitude associated with Rutherford scattering is

$$t_C = -\delta_{mm'}\delta_{MM'} \frac{2p\eta_C}{q^2} \exp \left[-i\eta_C \ln \left(\frac{q^2}{4p^2} \right) + 2i\sigma_0 \right], \quad (\text{A3})$$

where

$$\sigma_0 = \arg \Gamma(1+i\eta_C), \quad \eta_C = \left(\frac{M_p}{E_d} \right)^{1/2} \alpha, \quad (\text{A4})$$

$$t_{XD} = g_x \sqrt{12\pi} \frac{q^2}{\kappa^2} \sum_{\mu M_s m_n} (-1)^{M+M'+M_s} \left[\begin{matrix} \frac{1}{2} & \frac{1}{2} & 1 \\ m & m_n & -M_s \end{matrix} \right] \left[\begin{matrix} \frac{1}{2} & \frac{1}{2} & 1 \\ m' & m_n & -M \end{matrix} \right] \left[\begin{matrix} 1 & 2 & 1 \\ M_s & \mu & -M' \end{matrix} \right] Y_{2\mu}^*(\hat{q}_1) \\ + \left[\begin{matrix} \frac{1}{2} & \frac{1}{2} & 1 \\ m & m_n & -M' \end{matrix} \right] \left[\begin{matrix} \frac{1}{2} & \frac{1}{2} & 1 \\ m' & m_n & -M_s \end{matrix} \right] \left[\begin{matrix} 1 & 2 & 1 \\ M_s & \mu & -M \end{matrix} \right] Y_{2\mu}(\hat{q}_2), \quad (\text{A8})$$

where the exchange pole is

$$g_x = -\frac{3m_p\gamma_0^2}{4\pi p^2(z-z_p)}, \quad (\text{A9})$$

and $\mathbf{q}_1 = \mathbf{p} + \mathbf{p}'/2$, $\mathbf{q}_2 = \mathbf{p}/2 + \mathbf{p}'$,

$$|q_1| = |q_2| = p \left(\frac{z}{4} + z \right)^{1/2}. \quad (\text{A10})$$

The S -state coupling constant is chosen to be $\gamma_0 = 1.656$, a value consistent with the triplet effective range parameter $R = 1.75$ fm (Ref. 9).

The nucleon triangle rescattering amplitude again contains both $l=0$ and 2 deuteron vertex functions. They are combined with a nucleon-nucleon scattering amplitude that is parametrized as

and

$$\mathbf{q} = \mathbf{p}' - \mathbf{p}, \quad q^2 = 2p^2(1 - \cos\theta), \quad (\text{A5})$$

with p the center of mass momentum (primed in the outgoing channel), q the momentum transfer, and $\alpha = \frac{1}{137}$ is the fine structure constant.

The neutron-exchange amplitude contains both $l=0$ and 2 components, separated as (using $\bar{\eta} = P\eta$ throughout)

$$t_X = t_{XS} + t_{XD}\bar{\eta}. \quad (\text{A6})$$

These amplitudes are, respectively,

$$t_{XS} = g_x (-1)^{M+M'} \sum_{m_n} \left[\begin{matrix} \frac{1}{2} & \frac{1}{2} & 1 \\ m & m_n & -M' \end{matrix} \right] \left[\begin{matrix} \frac{1}{2} & \frac{1}{2} & 1 \\ m' & m_n & -M \end{matrix} \right] \quad (\text{A7})$$

and

$$t_{NN} = a + b\boldsymbol{\sigma}_1 \cdot \hat{\mathbf{q}} \boldsymbol{\sigma}_2 \cdot \hat{\mathbf{q}}. \quad (\text{A11})$$

Although traditionally determined from nucleon-nucleon scattering, the coefficients a and b will be two of the variable parameters in the fitting process. The amplitude arising from the S -state vertex is taken to be

$$t_{\Delta S} = g_{\Delta} (a\delta_{mm'}\delta_{MM'} + bt_{\Delta_1}), \quad (\text{A12})$$

where

$$g_{\Delta} = \frac{\gamma_0^2}{4\pi q} \sin^{-1} \left[\frac{q}{(q^2 + 16\kappa^2)^{1/2}} \right] \quad (\text{A13})$$

is the spin averaged form given by Locher and Mitsu-tani,²⁷ and

$$t_{\Delta_1} = -\frac{6q^2}{\kappa^2} \sum_{\mu_1\mu_2} \left[\begin{matrix} 1 & 1 & 1 \\ -M & M' & -\mu_2 \end{matrix} \right] \left[\begin{matrix} \frac{1}{2} & \frac{1}{2} & 1 \\ m & -m' & \mu_1 \end{matrix} \right] Y_{1\mu_1}^*(\hat{\mathbf{q}}) Y_{1\mu_2}^*(\hat{\mathbf{q}}) (-1)^{M'-m'-1/2}. \quad (\text{A14})$$

The D -state vertex is included as an integration, through

$$t_{\Delta D} = (at_{\Delta_2} + bt_{\Delta_3}), \quad (\text{A15})$$

where the amplitudes are

$$t_{\Delta_2} = -\left[\frac{3}{4\pi} \right]^{1/2} \gamma_0^2 \delta_{mm'} \sum_{\mu} f_{\Delta\mu} \left[(-1)^{M'} \left[\begin{matrix} 1 & 2 & 1 \\ M & \mu & -M' \end{matrix} \right] + (-1)^M \left[\begin{matrix} 1 & 2 & 1 \\ M' & \mu & -M \end{matrix} \right] \right], \quad (\text{A16})$$

$$\begin{aligned}
t_{\Delta_3} = & 6 \left(\frac{3}{4\pi} \right)^{1/2} \gamma_0^2 \sum_{\mu_1 \mu_2 \mu_s} f_{\Delta\mu} (-1)^{M'-m'} \begin{pmatrix} \frac{1}{2} & 1 & \frac{1}{2} \\ -m' & \mu_1 & m \end{pmatrix} \\
& \times \begin{pmatrix} (-1)^{M_s-1/2} \begin{pmatrix} 1 & 1 & 1 \\ -M & M_s & -\mu_2 \end{pmatrix} \begin{pmatrix} 1 & 2 & 1 \\ M_s & \mu & -M' \end{pmatrix} \\
& + (-1)^{M+1/2} \begin{pmatrix} 1 & 1 & 1 \\ M_s & -M' & \mu_2 \end{pmatrix} \begin{pmatrix} 1 & 2 & 1 \\ M_s & \mu & -M \end{pmatrix} \end{pmatrix} Y_{l\mu_1}^*(\hat{q}) Y_{l\mu_2}^*(\hat{q}) . \quad (\text{A17})
\end{aligned}$$

The integral $f_{\Delta\mu}$ is given by

$$\begin{aligned}
f_{\Delta\mu} = & Y_{2\mu}(\hat{q}) \frac{1}{2\pi q} \int_0^\infty dy \frac{y}{y^2 + \kappa^2} \Phi_d(y) \\
& \times Q_2 \left[\frac{y^2 + \kappa^2 + q^2/4}{qy} \right], \quad (\text{A18})
\end{aligned}$$

where Q_2 is a Legendre function of the second kind. The deuteron wave function was taken from Yamaguchi and Yamaguchi,⁵³ and is

$$\Phi_d(q) = \frac{c_d q^2}{(q^2 + \gamma^2)^2}, \quad (\text{A19})$$

where $c_d = -2.828 \text{ fm}^{-2}$ and $\gamma = 309.44 \text{ MeV}$.

The amplitudes given above [Eqs. (A3), (A6), (A12), and (A15)] are general and can be simplified for any elastic scattering observable. In the particular case of σT_{22} , keeping only terms to first order in their $l=2$ contribution, we obtain

$$\begin{aligned}
(\sigma T_{22})' = & N (bP_1 + b^2P_2 + \bar{\eta}P_3 + a\bar{\eta}P_4 \\
& + b\bar{\eta}P_5 + a^2P_6 + aP_7), \quad (\text{A20})
\end{aligned}$$

where the adjustable parameters have been factored out. The normalization to units of mb/sr is $N = 10(\hbar c)^2 = 3.89 \times 10^5$. The individual terms are

$$\begin{aligned}
P_1 = & \frac{1}{3\sqrt{10}\pi} g_x \left[\frac{q^2}{\kappa^2} g_\Delta + \frac{\gamma_0^2 f_\Delta}{8\pi\sqrt{2}} \right] Y_{22}(\hat{q}), \\
P_2 = & \frac{3}{4\pi\sqrt{10}\pi} \frac{q^2}{\kappa^2} g_\Delta \left[\frac{q^2}{\kappa^2} q_\Delta + \frac{\sqrt{3}}{\pi\sqrt{2}} \gamma_0^2 f_\Delta \right] Y_{22}(\hat{q}), \\
P_3 = & -\frac{\sqrt{\pi}}{3\sqrt{5}} \frac{q^2}{\kappa^2} g_x \left(\frac{5}{2} \text{Reg}_C + g_x \right) Y_{22}(\hat{q}), \\
P_4 = & -\frac{\sqrt{5}\pi}{6} \frac{q^2}{\kappa^2} g_x g_\Delta Y_{22}(\hat{q}), \quad (\text{A21}) \\
P_5 = & \frac{1}{24\sqrt{5}\pi} \frac{q^2}{\kappa^2} g_x g_\Delta (9p^2 - 5q^2) Y_{22}(\hat{q}), \\
P_6 = & \frac{1}{\sqrt{\pi}} \gamma_0^2 g_\Delta f_\Delta Y_{22}(\hat{q}), \\
P_7 = & \frac{\gamma_0^2}{\sqrt{\pi}} f_\Delta \left[\text{Reg}_C + \frac{1}{\sqrt{3}} g_x \right] Y_{22}(\hat{q}),
\end{aligned}$$

where g_C is the Rutherford amplitude of Eq. (A3) without the $\delta_{mm'}\delta_{MM'}$ factor.

The pion-exchange diagram is assumed to contain both $l=0$ and 2 parts. Since it is the most distant diagram considered, only the shape of its interference with the neutron-exchange diagram is included. The pion-exchange amplitude is taken only in spin-averaged form,²⁷

$$g_\pi = \frac{1}{q_2} \sin^{-1} \left\{ \frac{q_2}{[q_2^2 + (\kappa + m_\pi)^2]^{1/2}} \right\}. \quad (\text{A22})$$

Because of its importance for the shape of the polarized cross section near $z = -1$, we also included a term for the interference of the exchange diagram with the background. With arbitrary magnitude and phase, the contributions to the polarized cross section of the smooth background and the interference of the neutron-exchange diagram with the background and the pion exchange diagram are

$$\sigma T_{22} = (\sigma T_{22})' + cP_8 + dP_9 + eP_{10}, \quad (\text{A23})$$

where

$$\begin{aligned}
P_8 = & g_x g_\pi (1 - z^2), \\
P_9 = & g_x (1 - z^2), \quad (\text{A24}) \\
P_{10} = & \frac{1}{p^2} (1 - z^2),
\end{aligned}$$

and c , d , and e are adjustable parameters.

The form given by Eq. (A23) contains six free parameters which can be adjusted to reproduce the polarized cross section. They include η , the value of the D -state normalization we seek. While a more complicated form could have been tried, it was anticipated that it would be difficult for the measurements to determine more than six free parameters. The polynomial series itself contains at most five.

APPENDIX B: THE METHOD OF ASYMPTOTICAL COEFFICIENTS

The angle extrapolation technique, which we have examined in this paper, has shortcomings which we have discussed at length. First, this method requires extrapolating an observable into a region where higher-order polynomials grow in an unbounded manner. Second, truncation errors, which are extremely difficult to estimate, have been shown to be large relative to experimental errors. Fi-

nally, as we have mentioned in Sec. IV, the neutron-exchange "pole" becomes a branch cut when Coulomb distortions are included. This means that the extrapolation function is no longer analytic at the pole position. Borbély has suggested an alternative to angle extrapolation, which he terms the "method of asymptotical coefficients,"²⁶ or MAC. In this appendix we will examine the use of this method.

For the sake of simplicity, we neglect for the moment the Coulomb distortion effects; we will also neglect some overall normalization factors in order to introduce the basic features of the method. The angle extrapolation method involves the construction of a function $F_2(z)$,

$$F_2(z) = (z - z_p)^2 \sigma T_{22}. \quad (\text{B1})$$

The $(z - z_p)^2$ factor removes the double pole in the cross section at the (unphysical) angle corresponding to z_p . We can expand the function F_2 in a set of orthonormalized polynomials $\{P_l\}$,

$$F_2(z) = \sum_{l=0}^L a_l P_l(z) + \sum_{l=L+1}^{\infty} a_l P_l(z). \quad (\text{B2})$$

In Eq. (B2), L is the highest value for which the coefficients a_l can be reliably determined for a given set of measurements; i.e., for $l > L$,

$$\left| \frac{\delta a_l}{a_l} \right| \approx 1, \quad (\text{B3})$$

where δa_l is the error associated with the coefficient a_l . The second term in Eq. (B2), which cannot be determined from a given set of data, is called the truncation error in F_2 .

The coefficient η is determined by extrapolation of F_2 to the unphysical angle z_p :

$$\begin{aligned} F_2(z_p) &\equiv \eta = \sum_{l=0}^{\infty} a_l P_l(z_p) \\ &= \sum_{l=0}^L a_l P_l(z_p) + \sum_{l=L+1}^{\infty} a_l P_l(z_p). \end{aligned} \quad (\text{B4})$$

Clearly, since the last term in Eq. (B4) cannot be determined from the measurements, determination of η by extrapolation suffers from the problem of truncation error. This method also suffers because F_2 is not analytic at z_p , due to the branch cut caused by the Coulomb corrections. The "method of asymptotical coefficients" is an attempt to determine η while avoiding at least some of these difficulties.

The MAC involves the definition of an auxiliary function $F_1(z)$

$$F_1(z) = (z - z_p) \sigma T_{22}, \quad (\text{B5})$$

which has a simple pole at z_p (it also has a branch cut beginning at z_p , but the pole term is basically unaltered). We can expand this function as well in the polynomials $\{P_l\}$ as

$$F_1(z) = \sum_{l=0}^{\infty} b_l P_l(z). \quad (\text{B6})$$

From Eqs. (B2) and (B4), we can write

$$F_2(z) = \eta + \sum_{l=0}^{\infty} a_l [P_l(z) - P_l(z_p)], \quad (\text{B7})$$

and therefore

$$F_1(z) = \frac{\eta}{z - z_p} + \sum_{l=0}^{\infty} a_l \left[\frac{P_l(z) - P_l(z_p)}{z - z_p} \right]. \quad (\text{B8})$$

The first order pole in F_1 is seen explicitly in Eq. (B8). If, in the expansion of F_2 , $a_l \approx 0$ for all $l > \mathcal{L}$ then we can write

$$F_2(z) \approx \eta + \sum_{l=0}^{\mathcal{L}} a_l [P_l(z) - P_l(z_p)] \quad (\text{B9})$$

and

$$F_1(z) \approx \frac{\eta}{z - z_p} + \sum_{l=0}^{\mathcal{L}} a_l \left[\frac{P_l(z) - P_l(z_p)}{z - z_p} \right]. \quad (\text{B10})$$

We can expand the pole term in Eq. (B9) in terms of the same polynomials,

$$\frac{1}{z - z_p} = \sum_{l=0}^{\infty} c_l P_l(z); \quad (\text{B11})$$

therefore we have

$$F_1(z) \approx \eta \sum_{l=0}^{\infty} c_l P_l(z) + \sum_{l=0}^{\mathcal{L}} a_l \left[\frac{P_l(z) - P_l(z_p)}{z - z_p} \right]. \quad (\text{B12})$$

The last term in Eq. (B12) is a polynomial of degree $\mathcal{L} - 1$, so the assumption that the coefficients a_l vanish for $l > \mathcal{L}$ requires that

$$b_l = \eta c_l \quad \text{for } l \geq \mathcal{L}. \quad (\text{B13})$$

Consequently, the coefficient η can be obtained by comparing the high-order coefficients of a polynomial expansion of F_1 with the corresponding coefficients of $(z - z_p)^{-1}$.

Coulomb distortions in the initial and final states have two effects on the MAC. First, the coefficient η in Eq. (B9) gets replaced by an angle dependent function $\eta \mathcal{P}(z)$. Second, the nonpole terms in Eq. (B9) develop a branch cut at z_p . The function $\mathcal{P}(z)$ is analytic at z_p and can be expanded in a Taylor series about that point,

$$\mathcal{P}(z) = \mathcal{P}(z_p) + \sum_{l=1}^{\infty} \frac{1}{l!} (z - z_p)^l \mathcal{P}^{(l)}(z_p), \quad (\text{B14})$$

where $\mathcal{P}(z_p) = P$, the penetrability defined in Eq. (4), and $\mathcal{P}^{(l)}(z_p)$ is the l th derivative of \mathcal{P} evaluated at z_p . Absorbing the $l=1$ and higher terms of Eq. (B14), Eq. (B10) can be rewritten as

$$F_1(z) \approx \frac{\eta P}{z - z_p} + \sum_{l=1}^{\infty} a_l' \left[\frac{P_l(z) - P_l(z_p)}{z - z_p} \right]. \quad (\text{B15})$$

Therefore, the Coulomb effects require that the coefficients of the pole term be scaled by ηP , where P is the Coulomb penetrability.⁵⁴

The MAC has a superficial appeal. One never has to mention the word extrapolation; one can also imagine us-

ing this technique when the function is not analytic at the extrapolation point. However, both this method and the extrapolation technique have the same difficulty with truncation errors. Our demonstration of the relation between the extrapolation method and the MAC relied on the assumption that the truncation error was zero. However, if the truncation error is non-negligible, then the second term in Eq. (B8) will contribute higher order terms which will invalidate Eq. (B13).

To compare these two methods, we have applied them to determine η from many sets of $\bar{d} + p$ scattering data. We have almost always found the values obtained by the two techniques to be identical to within one standard deviation (frequently the two results are virtually equal). Therefore, the large truncation errors which we found in the extrapolation method should reappear with the MAC. To show the effects of truncation error for the MAC, we have used six data sets for $\bar{d} + p$ at energies from 10 to 56 MeV. Results for both conformal mapping and MAC are shown in Table VIII.

The MAC average is $\langle \eta \rangle = 0.0248 \pm 0.0008$, compared

with $\langle \eta \rangle = 0.0255 \pm 0.0005$ for the conformal mapping, using this subset of the data. These two results are completely consistent with one another, in agreement with our claim that these two methods are very similar. However, if we apply the pole suppression method to these same data, we obtain $\langle \eta \rangle = 0.0296 \pm 0.0010$. This value for $\langle \eta \rangle$ is six "standard deviations" from the MAC value, for exactly the same data base!

We conclude that the MAC exhibits the same defects as the conformal mapping procedure for $\bar{d} + p$. The two methods give results which are essentially equivalent, and both methods give serious underestimates of the truncation error. Note that if we had compared the MAC and conformal mapping to one another (without using our model or the pole suppression factor), we might have arrived at the quite erroneous conclusion that the agreement between these two values of $\langle \eta \rangle$ implied that the truncation errors were small. This further illustrates the limitations of attempting to deduce the truncation error by comparing different methods of extracting $\langle \eta \rangle$.²⁴

-
- ¹R. D. Amado, Phys. Rev. C **19**, 1473 (1979); J. L. Friar, *ibid.* **20**, 325 (1979).
²L. D. Knutson and W. Haeblerli, Phys. Rev. Lett. **35**, 558 (1975).
³R. C. Johnson and F. D. Santos, Part. Nucl. **2**, 285 (1971).
⁴K. Stephenson and W. Haeblerli, Phys. Rev. Lett. **45**, 520 (1980).
⁵R. P. Goddard, L. D. Knutson, and J. A. Tostevin, Phys. Lett. **118B**, 241 (1982).
⁶N. L. Rodning and L. D. Knutson, Phys. Rev. Lett. **57**, 2248 (1986).
⁷J. A. Tostevin and R. C. Johnson, Phys. Lett. **124B**, 135 (1983).
⁸R. D. Amado, M. P. Locher, and M. Simonius, Phys. Rev. C **17**, 403 (1978).
⁹R. D. Amado, M. P. Locher, J. Martorell, V. König, R. E. White, P. A. Schmelzbach, W. Gruebler, H. R. Bürgi, and B. Jenny, Phys. Lett. **79B**, 368 (1978).
¹⁰H. E. Conzett, F. Hinterberger, P. von Rossen, F. Seiler, and E. J. Stephenson, Phys. Rev. Lett. **43**, 572 (1979).
¹¹W. Gruebler, V. König, P. A. Schmelzbach, B. Jenny, and F. Sperisen, Phys. Lett. **92B**, 279 (1980).
¹²I. Borbély, V. König, W. Gruebler, B. Jenny, and P. A. Schmelzbach, Nucl. Phys. **A351**, 107 (1981); I. Borbély, W. Gruebler, V. König, P. A. Schmelzbach, and B. Jenny, Phys. Lett. **109B**, 262 (1982).
¹³J. M. Blatt and V. F. Weisskopf, *Theoretical Nuclear Physics* (Wiley, New York, 1952), Chap. 2.
¹⁴T. E. O. Ericson and M. Rosa-Clot, Annu. Rev. Nucl. Part. Sci. **35**, 271 (1985); this article contains an excellent summary of work on properties of the deuteron.
¹⁵T. E. O. Ericson and M. Rosa-Clot, Phys. Lett. **110B**, 193 (1982); Nucl. Phys. **A405**, 497 (1983); J. Phys. G **10**, L201 (1984).
¹⁶S. Klarsfeld, J. Martorell, and D. W. L. Sprung, Nucl. Phys. **A352**, 113 (1984).
¹⁷S. Klarsfeld, J. Martorell, and D. W. L. Sprung, J. Phys. G **10**, L165 (1984); **10**, 2205 (1984); **10**, L205 (1984).
¹⁸M. Lacombe, B. Loiseau, J. M. Richard, R. Vinh Mau, J. Côté, P. Pirès, and R. de Tourreil, Phys. Rev. C **2**, 861 (1980).
¹⁹J. T. Londergan, C. E. Price, and E. J. Stephenson, Phys. Lett. **120B**, 270 (1983).
²⁰D. D. Pun Casavant, J. G. Sowinski, and L. D. Knutson, Phys. Lett. **154B**, 6 (1985).
²¹M. P. Locher and T. Mizutani, J. Phys. G **4**, 287 (1978).
²²G. H. Berthold and H. Zankel, Phys. Rev. C **30**, 13 (1984).
²³I. Borbély, Phys. Lett. **160B**, 17 (1985).
²⁴I. Borbély, W. Gruebler, V. König, P. A. Schmelzbach, and B. Vuaridel (unpublished).
²⁵The nearest singularities give rise to the most rapid angular variation of the scattering amplitude.
²⁶I. Borbély, J. Phys. G **5**, 937 (1979).
²⁷M. P. Locher and T. Mizutani, Phys. Rep. **46**, 43 (1978).
²⁸F. D. Santos and P. C. Colby, Phys. Lett. **101B**, 291 (1981); Nucl. Phys. **A367**, 197 (1981).
²⁹P. C. Colby, Nucl. Phys. **A370**, 77 (1981).
³⁰K. Hatanaka, N. Matsuoka, H. Sakai, T. Saito, K. Hosono, Y. Koike, M. Kondo, K. Imai, H. Shimizu, T. Ichihara, K. Nisimura, and A. Okihana, Nucl. Phys. **A426**, 77 (1984).
³¹W. Gruebler, V. König, P. A. Schmelzbach, B. Jenny, H. R. Bürgi, P. Doleschall, G. Heidenreich, H. Roser, F. Seiler, and W. Reichart, Phys. Lett. **74B**, 173 (1978).
³²D. C. Kocher and T. B. Clegg, Nucl. Phys. **A132**, 455 (1969).
³³P. R. Bevington, *Data Reduction and Error Analysis for the Physical Sciences* (McGraw-Hill, New York, 1969).
³⁴The chi square value for the measurements at 20 MeV stabilized at 2.6 rather than 1.0 as a function of increasing L . This occurs because neighboring values of T_{22} are not smooth within the quoted errors. The errors in parentheses in Table I (and in all subsequent tables) take this into account by multiplying the statistical error by $(\chi^2/\nu)^{1/2}$, whenever this quantity is significantly greater than 1. The values of $d\eta$ in parentheses are used in determining the weighted average value $\langle \eta \rangle$. We differ from Ref. 11 in the choice of L for 20 MeV. The value of chi square continues to improve slowly

- for $L=2-5$. A choice of $L=2$ would have led to $\eta=0.0254\pm 0.0007$.
- ³⁵R. V. Reid, *Ann. Phys. (N.Y.)* **50**, 411 (1968).
- ³⁶In addition, the energy dependence introduced by the Coulomb correction makes the individual data points inconsistent with their own average. The reduced chi square for the average is 2.06 with the Coulomb correction and 1.15 without. In the Coulomb-corrected case, the weighted average and error have little meaning, since the assumption of statistical consistency is not satisfied.
- ³⁷In Ref. 38 an attempt was made to calculate an "improved" Coulomb penetrability correction by considering three-body reaction amplitudes with two charged particles. The corrections obtained by these authors are always smaller than the results from Ref. 28 (i.e., P is closer to 1 at all energies). In addition, for proton energies greater than 20 MeV the "Coulomb penetrability correction" is greater than 1. We have continued to use the values of P from Ref. 28.
- ³⁸A. M. Mukhamedzhanov, I. Borbély, W. Grüebler, V. König, and P. A. Schmelzbach, *Izv. Akad. Nauk USSR* **48**, 350 (1984).
- ³⁹Later in this paper we will optimize our model parameters by adjusting them to best reproduce the measured angular distributions, using the experimental errors for the weighting function. Then polynomial reproductions of the model will be made to simulate what happens when making real measurements. To maintain all such comparisons on a similar basis, and to be able to study the contribution of each expansion coefficient to the final value of η , we will use orthonormal polynomials throughout the rest of this paper.
- ⁴⁰F. James and M. Roos, *Comput. Phys. Commun.* **10**, 343 (1975).
- ⁴¹The errors listed for each parameter in Table II were obtained from the minimization procedure, which relies on the relative experimental errors. First, all the parameters were varied until the chi square was minimized. Then, each parameter was systematically moved away from its "best" value while the others were allowed to change freely. The "error" quoted for each parameter represents the amount by which that parameter could be moved before the chi square increased by 1. [In the case of the 20 MeV data, point-to-point variations were outside statistics, and the best value of χ^2/ν was 2.95. In this case, the error in each parameter was estimated by independently varying that parameter until χ^2/ν had increased by a factor of $(\chi^2/\nu)^{1/2}=1.72$.]
- ⁴²Locher and Mizutani (Ref. 21) obtained a value of $a=30.9$ (when their result is converted into our units) by fitting $n+d$ scattering at a neutron lab energy of 5.64 MeV.
- ⁴³It is important to check that approximations in model amplitudes other than g_x do not seriously perturb the determination of η . The value of η is given in the fit essentially as the coefficient of the P_3 term in Eq. (A20). This term contains the quantity g_x^2 [Eq. (A9)], which varies rapidly with z near $z=-1$, and produces the rapid changes in slope of σT_{22} near $z=-0.8$ (see Fig. 5). Other terms in the model are smoother near these values of z .
- ⁴⁴R. E. Cutkosky and B. B. Deo, *Phys. Rev.* **174**, 1859 (1968).
- ⁴⁵The ${}^2\text{H}(d,p){}^3\text{H}$ data differ from the $d+p$ elastic data, since in the former reaction there is no Rutherford singularity at forward angles. In this sense, that reaction is potentially "cleaner" than the $\bar{d}+p$ reaction. However, other corrections noted in this paper (the truncation error, the Coulomb penetrability correction, and the problem of the cut beginning at the nucleon-exchange singularity) all occur as well for the ${}^2\text{H}(d,p){}^3\text{H}$ reaction. There is no *a priori* reason why truncation errors should not also be large for this reaction.
- ⁴⁶If we include Coulomb effects at the particle-exchange singularity, via a distorted wave Coulomb analysis (Refs. 28 and 38), the neutron exchange Born term (which gives a second-order pole in T_{22}) gets modified. The second-order pole remains, but becomes multiplied by an angle-dependent factor; this factor, evaluated at the unphysical angle z_p , gives the penetrability correction to η . The interference term between the neutron-exchange term and background terms in the cross section gives rise to cut terms.
- ⁴⁷E. J. Stephenson, H. E. Conzett, R. M. Larimer, B. T. Lee-man, R. Roy, and P. von Rossen, *Phys. Rev. C* **21**, 44 (1980).
- ⁴⁸W. Grüebler, V. König, P. A. Schmelzbach, F. Sperisen, B. Jenny, R. E. White, F. Seiler, and H. W. Roser, *Nucl. Phys.* **A398**, 445 (1983); R. E. White, W. Grüebler, B. Jenny, V. König, P. A. Schmelzbach, and H. R. Bürgi, *ibid.* **A321**, 1 (1979).
- ⁴⁹Attempts to use the measurements reported in the plots of Ref. 48 to directly confirm the extrapolations reported in Ref. 11 at the higher energies were unsuccessful by as much as a factor of 2. This is unfortunate since the original measurements used in Ref. 11 are not available for inspection.
- ⁵⁰W. Grüebler, V. König, P. A. Schmelzbach, B. Jenny, H. R. Bürgi, R. A. Hardekopf, J. Nurzynski, R. Risler, G. Heidenriech, F. Seiler, and H. W. Roser, *Nucl. Phys.* **A334**, 365 (1980).
- ⁵¹The successful observation of $0^+(d,\alpha)0^-$ reaction at 56 MeV has been reported by S. Kato, N. Matsuoka, K. Hatanaka, T. Noro, M. Nakamura, M. Yosoi, and T. Ichihara, *Research Center for Nuclear Physics (Osaka) Annual Report*, 1983, p. 40.
- ⁵²M. Jacob and G. C. Wick, *Ann. Phys. (N.Y.)* **7**, 404 (1959).
- ⁵³Y. Yamaguchi and Y. Yamaguchi, *Phys. Rev.* **95**, 1635 (1954).
- ⁵⁴We have simplified here the actual procedure which is carried out. For example, the "optimal conformal mapping" procedure is frequently applied to the data before fitting, and both F_1 and F_2 are usually expanded using (different) sets of orthogonal polynomials constructed from the data. This last step has the advantage that coefficients of each polynomial are independent of one another, and that by definition the statistical error for each coefficient is ± 1 . Finally, we disagree with Borbély, who excludes the penetrability P in the first term of Eq. (B15).